

Experimental investigation of carbon steel and stainless steel bolted connections at different strain rates

Yancheng Cai^{*1} and Ben Young^{2a}

¹ Department of Civil Engineering, The University of Hong Kong, Pokfulam Road, Hong Kong

² Department of Civil and Environmental Engineering, The Hong Kong Polytechnic University, Hong Kong
(Formerly, Department of Civil Engineering, The University of Hong Kong, Pokfulam Road, Hong Kong)

(Received January 9, 2019, Revised March 5, 2019, Accepted March 10, 2019)

Abstract. A total of 36 carbon steel and stainless steel bolted connections subjected to shear loading at different strain rates was experimentally investigated. The connection specimens were fabricated from carbon steel grades 1.20 mm G500 and 1.90 mm G450, as well as cold-formed stainless steel types EN 1.4301 and EN 1.4162 with nominal thickness 1.50 mm. The connection tests were conducted by displacement control test method. The strain rates of 10 mm/min and 20 mm/min were used. Structural behaviour of the connection specimens tested at different strain rates was investigated in terms of ultimate load, elongation corresponding to ultimate load and failure mode. Generally, it is shown that the higher strain rate on the bolted connection specimens, the higher ultimate load was obtained. The ultimate loads were averagely 2-6% higher, while the corresponding elongations were averagely 8-9% higher for the test results obtained from the strain rate of 20 mm/min compared with those obtained from the lower strain rates (1.0 mm/min for carbon steel and 1.5 mm/min for stainless steel). The connection specimens were generally failed in plate bearing of the carbon steel and stainless steel. It is shown that increasing the strain rate up to 20 mm/min generally has no effect on the bearing failure mode of the carbon steel and stainless steel bolted connections. The test strengths and failure modes were compared with the results predicted by the bolted connection design rules in international design specifications, including the Australian/New Zealand Standard (AS/NZS4600 2018), Eurocode 3 - Part 1.3 (EC3-1.3 2006) and North American Specification (AISI S100 2016) for cold-formed carbon steel structures as well as the American Specification (ASCE 2002), AS/NZS4673 (2001) and Eurocode 3 - Part 1.4 (EC3-1.4 2015) for stainless steel structures. It is shown that the AS/NZS4600 (2018), EC3-1.3 (2006) and AISI S100 (2016) generally provide conservative predictions for the carbon steel bolted connections. Both the ASCE (2002) and the EC3-1.4 (2015) provide conservative predictions for the stainless steel bolted connections. The EC3-1.3 (2006) generally provided more accurate predictions of failure mode for carbon steel bolted connections than the AS/NZS4600 (2018) and the AISI S100 (2016). The failure modes of stainless steel bolted connections predicted by the EC3-1.4 (2015) are more consistent with the test results compared with those predicted by the ASCE (2002).

Keywords: bearing failure; bolted connection; carbon steel; experimental investigation; strain rate; stainless steel

1. Introduction

Cold-formed steel structural members, such as beams, columns and tension members are commonly assembled by bolt connections in construction. Structural behaviour of carbon steel bolted connections (Rogers and Hancock 1998, Rogers and Hancock 1999, Chung 2005, Teh and Clements 2012, Teh and Uz 2015) and stainless steel bolted connections (Kim and Kuwamura 2007, Bouchaïr *et al.* 2008, Salih *et al.* 2010, 2011, Cai and Young 2014a) subjected to shear loading have been extensively investigated. Design specifications of carbon steel and stainless steel bolted connections subjected to shear loading are currently available, such as the Australian/New Zealand Standard (AS/NZS4600 2018) for Cold-formed Steel

Structures, Eurocode 3 - Design of Steel Structures - Part 1.3 (EC3-1.3 2006): General Rules - Supplementary Rules for Cold-formed Members and Sheeting, the North American Specification (AISI S100 2016) for the Design of Cold-formed Steel Structural Members, the American Society of Civil Engineers Specification (ASCE 2002) for the Design of Cold-formed Stainless Steel Members, the Australian/New Zealand Standard (AS/NZS4673 2001) for Cold-formed Stainless Steel Structures and the Eurocode 3 - Design of Steel Structures - Part 1.4 (EC3-1.4 2015): General Rules - Supplementary Rules for Stainless Steels. They are applicable for room (ambient) temperature conditions, but not for high temperature conditions. In the past few years, over hundreds of experimental tests and numerical models on bolted connections of carbon steel (Yan and Young 2011, 2012, 2013) and stainless steel (Cai and Young 2014b, c, 2015) at elevated temperature were conducted. Subsequently, design rules were proposed for bolted connections of carbon steel (Yan and Young 2012) and stainless steel (Cai and Young 2018) subjected to bearing failure of connection plates at elevated

*Corresponding author, Post-doc Fellow,
E-mail: yccai@hku.hk

^a Professor, E-mail: ben.young@polyu.edu.hk

temperatures.

In addition to the bolted connections subjected to shear loading, the structural behaviour of bolted connections subjected to cyclic loading conditions have been investigated, e.g., bolted connections in steel beam-columns (Vatansever and Kutsal 2018, Kazemi *et al.* 2018) and bolted connections in composite structures (Li *et al.* 2017a, b, 2018). For the bolted connection in steel beam-column joints, a modified component method for the mechanical behaviour was proposed by Kazemi *et al.* (2018); while for the bolted connections involving concrete filled steel columns, the shear transfer mechanism was investigated by De Nardin and El Debs (2018). In these research works, the commonly used steel bolts with steel nuts were applied. Innovative solutions for bolted connections in steel and composite structures were also investigated, e.g., demountable steel column-column bolted connections (Li *et al.* 2016) and blind bolted connections in concrete filled steel tubular columns (Agheshlui *et al.* 2017).

The above researches mainly looked into the bolted connections under static loading conditions, namely, the tests of the bolted connections were conducted at relatively low strain rate, e.g., 1.0 mm/min (0.017 mm/s) by Yan and Young (2011) and 0.5 mm/min (0.0083 mm/s) by Li *et al.* (2017a). It should be noted that effects of strain rate on behaviour of steel and composite structures have received much attention as there is an increasing need to design structures under accidental dynamic loads, e.g., impact loadings and seismic conditions. Esaki and Ono (2001) studied the effects of strain rate (up to 10 mm/s) on mechanical behavior of SRC shearwalls. Boh *et al.* (2004) investigated the strain rate effects on the response of stainless steel corrugated firewalls subjected to hydrocarbon explosions. Research on the mechanical properties of structural steel (Soroushian and Choi 1987) and thin sheet steel (Pan *et al.* 2001) at different strain rates showed that all the characteristic stress and strain values increase with increasing strain rate, and steel with lower yield strength is more sensitive to strain rate. Structural behaviour of steel members subjected to impact loads was investigated by Jones (1997), Lu and Yu (2003), Zeinoddini *et al.* (2002, 2008), Rathnaweera *et al.* (2011) and Yuen *et al.* (2011). Effect of strain rates on behaviour of welded steel beam-to-column connections was analysed by El Hassouni *et al.* (2011). Previous research works have shown that the loading or deformation rate is a parameter that significantly influences the joint behaviour, e.g., nailed timber joints (Girhammar and Andersson 1988) and bolted end-plate joints of steel (Grimsno *et al.* 2015). However, it should be noted that there is limited investigation on the effects of strain rate on bolted connections of carbon steel and stainless steel subjected to shear loading up to date, which is the main focus of this study.

In this study, structural behaviour of bolted connections fabricated from carbon steel and stainless steel were experimentally investigated at different strain rates. The connection specimens were fabricated from carbon steel grades 1.20 mm G500 and 1.90 mm G450, as well as cold-formed stainless steel types EN 1.4301 and EN 1.4162 with nominal thickness 1.50 mm. Totally 36 bolted connection

specimens were designed and tested, including 15 series for carbon steel and 5 series for stainless steel. The connection specimens were subjected to tensile loading by displacement control test method. Different strain rates of 10 mm/min and 20 mm/min were used in the connection tests. The structural behaviour of the same series of connection specimens under different strain rates was investigated in terms of ultimate load, elongation corresponding to ultimate load and failure mode. In addition, the current international design rules for carbon steel and stainless steel bolted connections were assessed by comparing with the test results. The purpose of this paper is to present the effects of strain rate on the structural behaviour of carbon steel and stainless steel bolted connections that subjected to shear loading.

2. Experimental investigation

2.1 Specimen design

The carbon steel and stainless steel were used to fabricate the bolted connection specimens. The carbon steel included the grades of G450 and G500, with the respective nominal thicknesses (t) of 1.90 mm and 1.20 mm. The stainless steel included austenitic stainless steel type EN 1.4301 and lean duplex stainless steel type EN 1.4162, with both $t = 1.50$ mm. For simplicity, the stainless steel types EN 1.4301 and EN 1.4162 have been shortened as types A and L, respectively, hereafter in this paper.

Totally 20 series of connection specimens including 15 series for carbon steel and 5 series for stainless steel were designed, which varied in plate thickness, steel grades, bolt diameters and bolt numbers. The carbon steel connection plates were machined from the thin sheets in the longitudinal direction, which were consistent with the coupon specimens. The stainless steel connection plates were cut from the tubes with nominal section dimensions of 50×20×1.5 in mm. The nominal width (w) of the connection plates was kept as 50 mm. The connection plates were designed carefully such that the assembled connection specimens would mainly fail by plate bearing that referring to the previous test results of carbon steel bolted connections conducted by Yan and Young (2011, 2013) and stainless steel bolted connections conducted by Cai and Young (2014a). The connection specimens in single shear were bolted with two steel plates while double shear with three steel plates. The two plates for single shear connection specimen had either identical thickness or different thickness, while the three plates for double shear connection specimens had identical thickness. The total length of approximate 690 mm was used for each bolted connection specimen by varying the length of steel plates from 372 to 415 mm. The connection specimen was gripped at each end with a length of 65 mm (Yan and Young 2011, Cai and Young 2014a). Therefore, the clear length of 560 mm between two grips after assembling was maintained for each connection specimen. It should be noted that, for stainless steel connection plates, the lip of 10 mm in height was designed in the overlapped connection region to prevent the

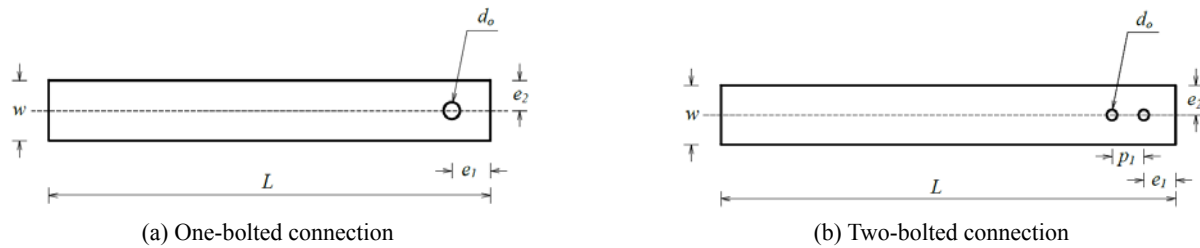


Fig. 1 Configurations of and symbols of connection plates

out-of-plane curling (Cai and Young 2014a), except for the middle plates in double shear connections. The notations of plate dimension are illustrated in Fig. 1. The nominal values of the notations for each steel plate are shown in Table 1.

The connection plate was designed with one bolt hole or two bolt holes in the parallel direction, as shown in Fig. 1. High strength steel bolts with Grade 12.9 (Yan and Young 2011) and stainless steel A4-80 bolts (Cai and Young 2014a) were used to assemble the carbon steel and stainless steel plates, respectively. Four sizes of bolts were used, namely, the M6, M8, M10 and M12 bolts. Steel washers and nuts in accordance with the bolts were used. The steel washers were used in both sides of the connection specimens. The nominal diameter of bolt hole (d_o) in the steel plate was drilled 1 mm larger than the nominal diameter of the bolt (d) if $d < 12$ mm, according to the carbon steel standards (AS/NZS4600 2018) and stainless

by hand-tightened to a torque of approximately 10 Nm for all the connection specimens, which allowed initial slip in the bolted connection at a small load level. Similar assembled criterion was used by Rogers and Hancock (1998), Yan and Young (2011) as well as Cai and Young (2014a).

The spacing requirements in the connected part of the bolted connections as specified in the carbon steel standards (AS/NZS4600 2018, EC3-1.3 2006, AISI S100 2016) and stainless steel standards (ASCE 2002, AS/NZS4673 2001, EC3-1.4 2015) are presented in Table 3. All the carbon steel and stainless steel bolted connection specimens could satisfy these requirements in this study. It should be noted that the spacing in the connection plates were designed such that the assembled connection specimens were mainly failed in plate bearing based on the design calculations.

2.2 Specimen labelling

The connection specimen was identified by the label indicating the connection type, material, bolt number and bolt diameter (d). The label of each connection specimen had four or five segments, depending on the connection types of single shear or double shear. It should be noted that the carbon steel of grades G450 and G500 having the nominal thicknesses of 1.90 mm and 1.20 mm, respectively, and the austenitic stainless steel EN 1.4301 and lean duplex stainless steel EN 1.4162 were shortened by A and L, respectively.

For examples of specimens “S-120-190-2-6” and “D-A-1-10”, the first segment indicates the connection type, “S” for single shear and “D” for double shear. The following segment shows the material of the connection specimen, where “120” and “190” mean the carbon steel 1.20 mm G500 and 1.90 mm G450, respectively; and the “A” is short for austenitic stainless steel. If it is a carbon steel connection

Table 1 Nominal dimensions of steel plates for specimens in single shear (mm)

Steel grade	Bolt hole	t	e_1	e_2	p_1	L	d_o
G450	One	1.20	27	25	-	372	9
G450		1.20	33	25	-	378	11
G500		1.90	27	25	-	372	9
G500		1.20	33	25	-	378	11
G450	Two	1.90	21	25	21	377	7
G500		1.20	21	25	21	377	7
EN 1.4301		1.50	27	25	27	386	9

Table 2 Nominal dimensions of steel plates for specimens in double shear (mm)

Steel grade	Bolt hole	t	e_1	e_2	p_1	L	d_o
G450	One	1.90	45	25	-	390	9
G450		1.90	55	25	-	400	11
G500		1.20	45	25	-	390	9
G500		1.20	55	25	-	400	11
EN 1.4301	Two	1.50	55	25	-	400	11
EN 1.4162		1.50	70	25	-	415	14
G450		1.90	35	25	21	390	7
G500		1.20	35	25	21	390	7
EN 1.4301		1.50	45	25	27	404	9
EN 1.4162		1.50	45	25	27	404	9

Table 3 Spacing requirements for bolt connections in different specifications

Steel	Specification	e_1	e_2	p_1
Cold-formed carbon steel	AS/NZS4600 (2018)	$\geq 1.5d$	$\geq 1.5d$	$\geq 3.0d$
	EC3-1.3 (2006)	$\geq 1.0d_o$	$\geq 1.5d_o$	$\geq 3.0d_o$
	AISI S100 (2016)	$\geq 1.5d$	$\geq 1.5d$	$\geq 3.0d$
Cold-formed stainless steel	ASCE (2002)	$\geq 1.5d$	$\geq 1.5d$	$\geq 3.0d$
	AS/NZS4673 (2001)	$\geq 1.5d$	$\geq 1.5d$	$\geq 3.0d$
	EC3-1.4 (2015)	$\geq 1.2d_o$	$\geq 1.2d_o$	$\geq 2.2d_o$

Table 4 Material properties of carbon steel and stainless steel (Cai and Young 2019)

Material	Steel grade	E	$f_{0.2}$	f_u	ϵ_u	ϵ_f
		GPa	MPa	MPa	%	%
Carbon steel	G500	214	622	630	5.8	8.9
	G450	212	486	511	8.2	13.9
Stainless steel	EN 1.4301	199	403	647	50.4	56.9
	EN 1.4162	200	681	800	19.5	38.6

connection specimen in single shear, there are two segments that indicate the material of the two connection plates; otherwise, there is only one segment indicating the material of the connection plates as they are identical. The following number indicates the bolt number used in the specimen, where “1” means one bolt, and “2” for two bolts arranged parallel to the loading direction; The last part of the label shows the nominal diameter (d) of the bolt, where “6” stands for $d = 6$ mm, “10” means $d = 10$ mm. The last letter R means it is a repeated test specimen.

2.3 Material properties

Material properties of the carbon steel of grades G450 and G500 and, stainless steel types EN 1.4301 and EN 1.4162 were measured by tensile coupon tests. The dimension of the coupons was designed according to the Australian Standard (AS1391 2007). The coupons were cut in the longitudinal direction of the steel sheets and tubes. The gauge length and width of the coupons were 50 mm and 12.5 mm, respectively. Two linear strain gauges were

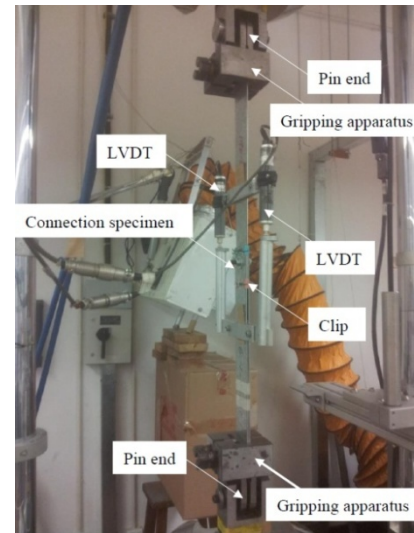


Fig. 2 Test setup of carbon steel double shear bolted connection

attached at the center of two surfaces in each coupon. In addition, a calibrated extensometer was used to measure the longitudinal strain during the tests. It should be noted that the zinc coating at the gauge length was removed in the carbon steel coupon specimens.

Two linear strain gauges were attached at the centres of two surfaces in each coupon. In addition, a calibrated extensometer was used to measure the longitudinal strain during the tests. The coupon tests were conducted in an MTS testing machine with 50 kN loading capacity. During the coupon tests, 90 seconds of pauses were made near the

Table 5 Test results of carbon steel bolted connections at different strain rates

Specimen series	Tests at different strain rates								
	1.0 mm/min*			10 mm/min			20 mm/min		
	t_m	$P_{u,1}$	$e_{elgn,1}$	t_m	$P_{u,10}$	$e_{elgn,10}$	t_m	$P_{u,20}$	$e_{elgn,20}$
	(mm)	(kN)	(mm)	(mm)	(kN)	(mm)	(mm)	(kN)	(mm)
S-120-120-1-8	1.24	18.52	11.55	1.24	20.00	11.03	1.22	19.87	10.99
S-120-120-1-10	1.22	19.72	9.42	1.22	20.05	11.16	1.22	21.85	11.71
S-120-120-1-10-R	-	-	-	1.24	20.78	-	-	-	-
S-120-190-1-8	1.23	20.48	10.55	1.24	20.34	10.28	1.23	20.20	10.43
S-120-190-1-10	1.24	22.15	11.25	1.23	24.27	11.87	1.22	23.51	10.98
S-190-190-1-8	1.92	25.47	12.54	1.91	26.17	14.09	1.91	26.30	16.02
S-190-190-1-10	1.91	27.74	12.34	1.92	28.40	12.73	1.92	30.21	14.92
S-120-120-2-6	1.22	27.47	9.73	1.23	27.07	10.95	1.23	28.07	9.35
S-120-190-2-6	1.22	28.70	8.55	1.22	29.38	8.63	1.21	29.60	7.79
S-190-190-2-6	1.92	31.70	5.80	1.92	33.71	7.92	1.91	34.92	7.18
D-120-1-8	1.22	21.91	8.68	1.23	23.32	10.28	1.24	22.33	11.14
D-120-1-10	1.23	24.79	10.18	1.22	25.12	9.58	1.23	25.01	10.97
D-190-1-8	1.92	33.54	12.97	1.92	35.68	14.82	1.91	35.67	15.11
D-190-1-10	1.92	38.39	14.01	1.93	39.32	13.75	1.92	38.90	13.05
D-120-2-6	1.23	30.25	7.54	1.23	30.45	7.46	1.22	30.65	7.33
D-190-2-6	1.91	41.51	7.67	1.92	43.20	9.50	1.92	43.62	8.41

*Note: Detailed in Cai and Young (2019)

Table 6 Test results and comparison of stainless steel bolted connections at different strain rates

Specimen series	Tests at different strain rates						Comparisons	
	1.5 mm/min*			20 mm/min			$P_{u,20}/P_u$	$e_{elgn,20}/e_{elgn}$
	t_m	P_u	e_{elgn}	t_m	$P_{u,20}$	$e_{elgn,20}$		
(mm)	(kN)	mm	(mm)	(kN)	(mm)			
S-A-2-8	1.46	38.24	19.27	1.42	38.60	19.52	1.01	1.01
D-A-1-10	1.42	34.52	18.34	1.42	35.14	15.02	1.02	0.82
D-L-1-12	1.46	44.38	10.33	1.45	46.37	18.60	1.04	1.80
D-A-2-8	1.43	42.08	16.25	1.43	41.62	14.44	0.99	0.89
D-L-2-8	1.45	52.96	7.52	1.45	54.83	7.70	1.04	1.02
						Mean	1.02	1.11
						COV.	0.022	0.357

*Note: Detailed in Cai and Young (2019)

0.2% proof stress ($f_{0.2}$), around the ultimate strength (f_u) and before the coupon fracture. This allowed the stress relaxation associated with plastic straining to take place. The initial average readings of the two strain gauges were used to determine the initial elastic Young's modulus (E). The details of the material properties of carbon steel and stainless steel are reported by Cai and Young (2019). Table 4 illustrates the material properties of E , $f_{0.2}$, f_u , the strain at ultimate strength (ϵ_u) and strain at fracture (ϵ_f).

2.4 Test rig and operation

The carbon steel and stainless steel bolted connection specimens were tested in an MTS universal testing machine. Two linear variable displacement transducers (LVDTs) were assembled in a frame that covers a distance of 200 mm in the middle part of the connection specimen. The elongation of the connection specimen was captured by the average readings of the LVDTs during the test. The specimen was assembled into the gripping apparatus at each end with a length of 65 mm. The gripping apparatus were purposely designed such that the tensile loading was applied either through the shear plane of the connection specimens in single shear or concentrically loaded for the connection specimens in double shear (Cai and Young 2014a). The gripping apparatus are free to rotate in one direction by pinned to the steel blocks that are subsequently fixed to the grips of the MTS testing machine. Clips linked with iron wire were used to prevent the extent of out-of-plane curling in the bolted connection part (Yan and Young 2011). The schematic views of the test setup are illustrated by Yan and Young (2011) and by Cai and Young (2014a). A typical test setup for carbon steel double shear bolted connection is shown in Fig. 2.

The bolted connection specimens were subjected to tensile loading by driving the actuator of the MTS testing machine. Displacement control test method was used in the connection tests. The strain rates of 10 mm/min and 20 mm/min were used for carbon steel bolted connections, while the 20 mm/min was used for stainless steel. The stainless steel bolted connections were tested under the higher strain rate of 20 mm/min only, due to the ductility of

stainless steel is higher than that of carbon steel, as shown in Table 4. The applied load and the readings of LVDTs were recorded in a data acquisition system during the tests.

3. Connection test results

Totally 36 tests of carbon steel and stainless bolted connection specimens were conducted in this study. The test results of the carbon steel and stainless steel bolted connections are shown in Tables 5 and 6, respectively. The thickness of the carbon steel and stainless steel plates for the bolted connection specimens were measured. For bolted connection specimens in single shear, the measured smaller thickness (t_m) of the connection plates were reported, while for specimens in double shear, the measured thickness (t_m) of the internal connection plates were reported. The $P_{u,10}$ and $P_{u,20}$ represent the ultimate loads of the bolted connections tested under the strain rates of 10 mm/min and 20 mm/min, respectively. The $e_{elgn,10}$ and $e_{elgn,20}$ mean the elongations corresponding to the $P_{u,10}$ and $P_{u,20}$, respectively. The elongation was measured at a distance of 200 mm in the middle part of the connection by the two LVDTs. The ultimate loads (P_u) and elongations (e_{elgn})

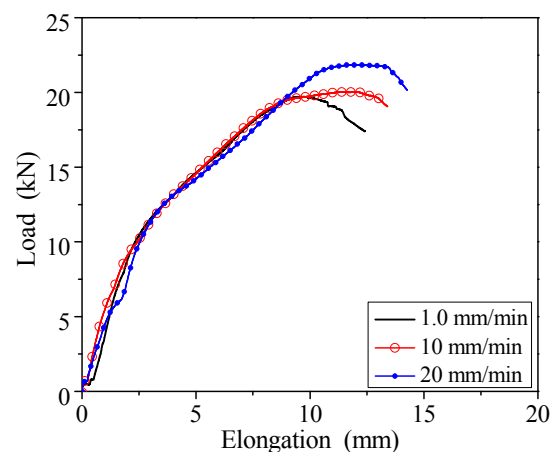


Fig. 3 Load-elongation curves of connection specimen Series S-120-120-1-10

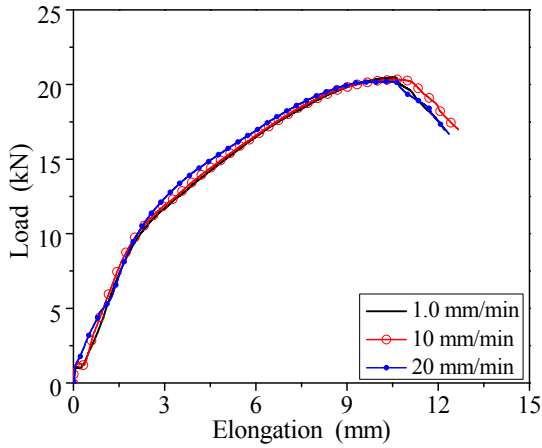


Fig. 4 Load-elongation curves of connection specimen Series S-120-190-1-8

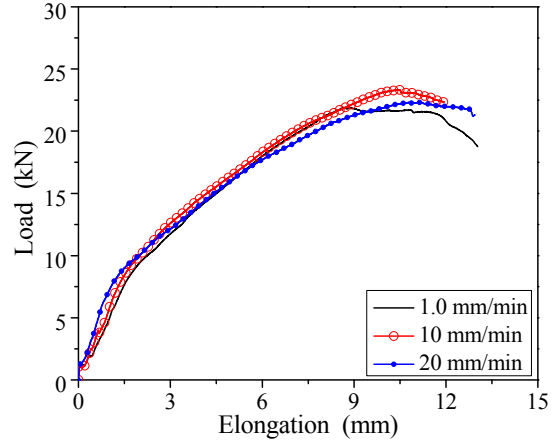


Fig. 7 Load-elongation curves of connection specimen Series D-120-1-8

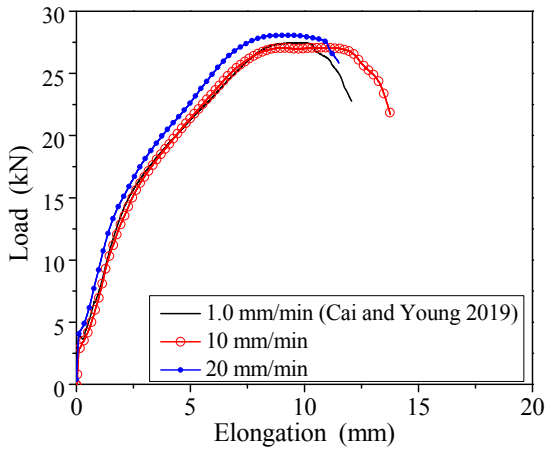


Fig. 5 Load-elongation curves of connection specimen Series S-120-120-2-6

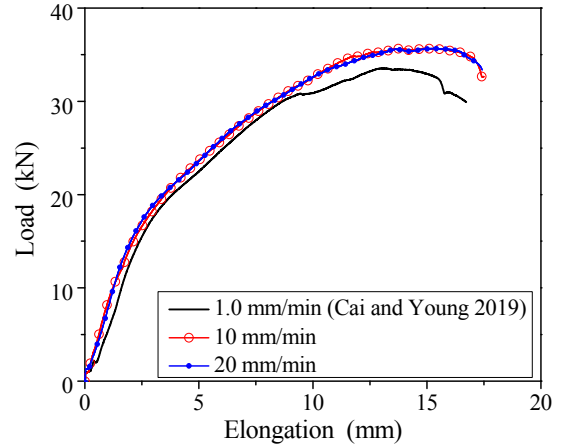


Fig. 8 Load-elongation curves of connection specimen Series D-190-1-8

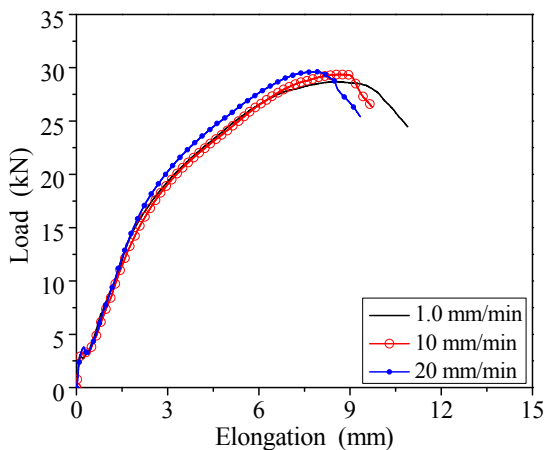


Fig. 6 Load-elongation curves of connection specimen Series S-120-190-2-6

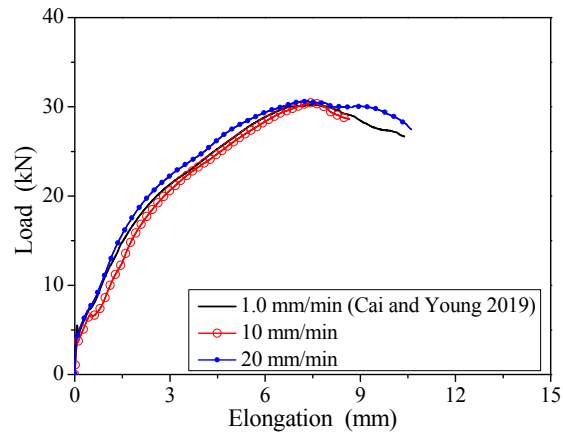


Fig. 9 Load-elongation curves of connection specimen Series D-120-2-6

corresponding to the ultimate loads of carbon steel and stainless steel bolted connections conducted at lower strain rates are also included, where the strain rates of 1.0 mm/min and 1.5 mm/min were respectively used for carbon steel and

stainless steel (Cai and Young 2019). The load-elongation test curves for single shear specimen series S-120-120-1-10, S-120-190-1-8, S-120-120-2-6 and S-120-190-2-6 are shown in Figs. 3-6, respectively; and for double shear specimen series D-120-1-8, D-190-1-8, D-120-2-6, D-190-

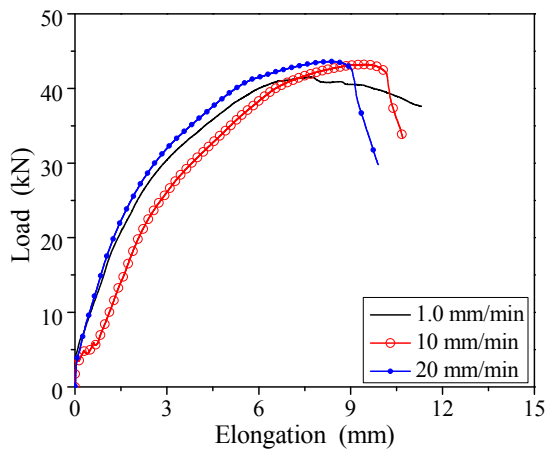


Fig. 10 Load-elongation curves of connection specimen Series D-190-2-6

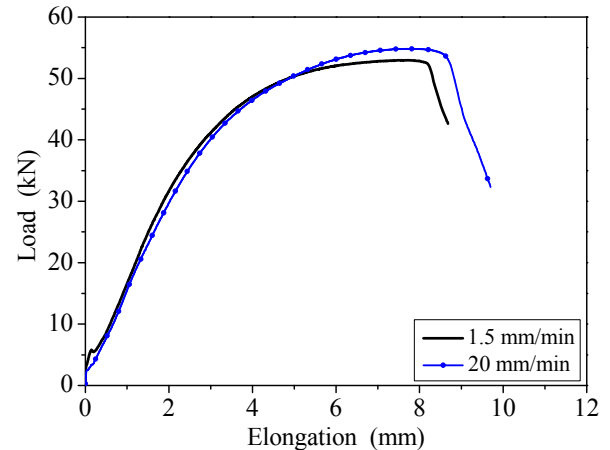


Fig. 11 Load-elongation curves of connection specimen Series D-L-2-8

2-6 and D-L-2-8 in Figs. 7-11, respectively. The vertical axis plotted the applied load on the specimen while the horizontal axis represented the elongation of the specimen. In the load-elongation curves, bolt slip displacement at small load level was shifted.

The failure modes of the carbon steel and stainless steel bolted connection specimens are shown in Tables 7 and 8, respectively. The definition of failure modes for carbon steel and stainless steel bolted connections follow the characteristics detailed by Yan and Young (2011) and by Cai and Young (2014a). The bolted connection specimens in this study were mainly failed in bearing failure (B) of the connection plates, except for specimen Series S-190-190-2-6

that failed in bolt shear (BS), Series D-L-2-8 that failed by net section tension (NS), and specimen series D-190-1-10 and D-190-2-6 that failed by net section tension (NS) failure mode undergoing higher strain rates. It should be noted that the failure modes of NS and tear out failure (end pull out) were deliberately avoided in the design of specimens, and they were not observed in the failed specimens at low strain rates (i.e., 1.0 mm/min for carbon steel and 1.5 mm/min for stainless steel). As mentioned earlier, the connection specimens were purposely designed to fail in bearing failure of the connection plates in this study. Note that for all the single shear bolted connection specimens, bolt tilting was observed as the elongation of the

Table 7 Test failure modes of carbon steel bolted connections at different strain rates and predicted failure modes

Specimen series	Tests at different strain rates			Predictions		
	1.0 mm/min*	10 mm/min	20 mm/min	AS/NZS4600 (2018)*	EC3-1.3 (2006)*	AISI S100 (2016)*
S-120-120-1-8	B	B	B	B	B	B
S-120-120-1-10	B	B	B	B	B	B
S-120-120-1-10-R	-	B	-	B	B	B
S-120-190-1-8	B	B	B	B	B	B
S-120-190-1-10	B	B	B	B	B	B
S-190-190-1-8	B	B	B	B	B	B
S-190-190-1-10	B	B	B	B	B	B
S-120-120-2-6	B	B	B	B	B	B
S-120-190-2-6	B	B	B	B	B	B
S-190-190-2-6	BS	BS	BS	-	-	-
D-120-1-8	B	B	B	B	B	B
D-120-1-10	B	B	B	NS	B	NS
D-190-1-8	B	B	B	B	B	B
D-190-1-10	B	NS	NS	NS	B	NS
D-120-2-6	B	B	B	NS	B	NS
D-190-2-6	B	NS	NS	NS	B	NS

*Note: Detailed in Cai and Young (2019); B = Bearing; BS = Bolt shear; NS = Net section tension

Table 8 Test failure modes of stainless steel bolted connections at different strain rates and predicted failure modes

Specimen series	Tests at different strain rates		Predictions	
	1.5 mm/min*	20 mm/min	ASCE (2002)*	EC3-1.4 (2015)*
S-A-2-8	B	B	NS	NS
D-A-1-10	B	B	NS	B
D-L-1-12	B	B	NS	B
D-A-2-8	B	B	NS	NS
D-L-2-8	NS	NS	NS	NS

*Note: Detailed in Cai and Young (2019); B = Bearing; NS = Net section tension

Table 9 Comparisons of ultimate loads and elongations for carbon steel bolted connections with different strain rates

Specimen series	Comparison of ultimate loads			Comparison of elongations		
	$P_{u,10}/P_u$	$P_{u,20}/P_u$	$P_{u,20}/P_{u,10}$	$e_{elgn,10}/e_{elgn}$	$e_{elgn,20}/e_{elgn}$	$e_{elgn,20}/e_{elgn,10}$
S-120-120-1-8	1.08	1.07	0.99	0.95	0.95	1.00
S-120-120-1-10	1.02	1.11	1.09	1.18	1.24	1.05
S-120-120-1-10-R	1.05	-	1.05	-	-	-
S-120-190-1-8	0.99	0.99	0.99	0.97	0.99	1.01
S-120-190-1-10	1.10	1.06	0.97	1.06	0.98	0.93
S-190-190-1-8	1.03	1.03	1.00	1.12	1.28	1.14
S-190-190-1-10	1.02	1.09	1.06	1.03	1.21	1.17
S-120-120-2-6	0.99	1.02	1.04	1.13	0.96	0.85
S-120-190-2-6	1.02	1.03	1.01	1.01	0.91	0.90
S-190-190-2-6	1.06	1.10	1.04	1.37	1.24	0.91
D-120-1-8	1.06	1.02	0.96	1.18	1.28	1.08
D-120-1-10	1.01	1.01	1.00	0.94	1.08	1.15
D-190-1-8	1.06	1.06	1.00	1.14	1.16	1.02
D-190-1-10	1.02	1.01	0.99	0.98	0.93	0.95
D-120-2-6	1.01	1.01	1.01	0.99	0.97	0.98
D-190-2-6	1.04	1.05	1.01	1.24	1.10	0.89
Mean	1.04	1.05	1.01	1.09	1.09	1.00
COV	0.030	0.035	0.034	0.112	0.127	0.100

connection specimen developed. The more obvious of tilting in bolts came along with the larger elongation of the connection specimens. This will be illustrated in the later section.

4. Effects of strain rates on bolted connections

4.1 Ultimate loads

The ultimate loads of the carbon steel and stainless steel bolted connection specimens obtained from the tests at different strain rates were compared, as shown in Tables 9 and 6, respectively. Generally, the connection specimens subjected to higher strain rates, the larger ultimate loads were obtained.

For carbon steel bolted connections (See Table 9), the

values of $P_{u,10}/P_u$ and $P_{u,20}/P_u$ are generally greater than 1.00. The mean values of the load ratio for $P_{u,10}/P_u$ and $P_{u,20}/P_u$ are 1.04 and 1.05, respectively, with the corresponding coefficients of variation (COV) of 0.030 and 0.035. The maximum values of load ratio for $P_{u,10}/P_u$ and $P_{u,20}/P_u$ are 1.10 and 1.11, respectively. The mean value of the load ratio for $P_{u,20}/P_{u,10}$ is 1.01 with the corresponding COV of 0.034. The mean value of $P_{u,20}/P_{u,10}$ is around 3% smaller than that of $P_{u,10}/P_u$ may indicate that as the strain rate in the connection tests become higher, the effects of strain rate on the ultimate loads of the connections becomes lower in this study. While for stainless steel bolted connections (See Table 6), it was found that the ultimate loads of $P_{u,20}$ are generally higher than those of P_u , except for Specimen Series D-A-2-9. The mean values of the load ratio for $P_{u,20}/P_u$ is 1.02 with the corresponding COV of 0.022. The maximum value of load ratio for $P_{u,20}/P_u$ is 1.04.

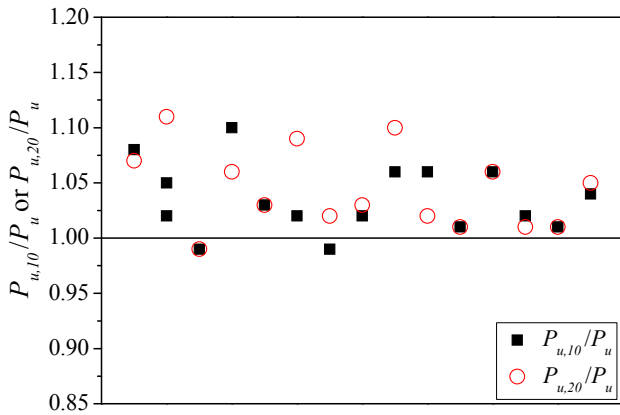


Fig. 12 Comparison of the ultimate loads for carbon steel bolted connections under different strain rates

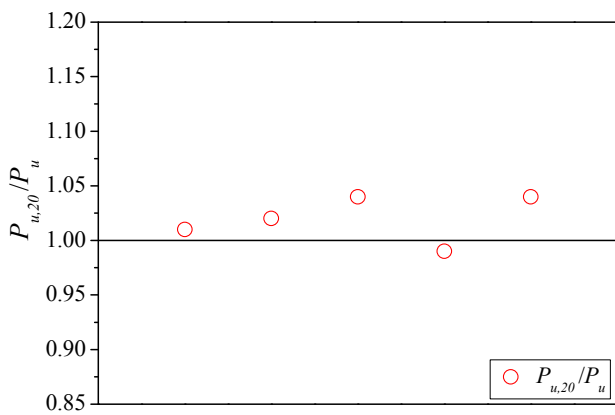


Fig. 13 Comparison of the ultimate loads for stainless steel bolted connections under different strain rates

Both the mean value and maximum value of $P_{u,20}/P_u$ for stainless steel bolted connections are smaller than those of carbon steel bolted connections. This may indicate that the effects of strain rates on the ultimate loads of stainless steel bolted connections were generally less significant than those of carbon steel bolted connections. The comparisons of the ultimate loads at different strain rates for carbon steel and stainless steel bolted connections are further illustrated in Figs. 12-13, respectively.

4.2 Elongations

The elongations at the ultimate loads for the carbon steel and stainless steel bolted connection specimens under different strain rates were also compared, as shown in Tables 9 and 6, respectively. For carbon steel bolted connections, the maximum values of the ratios for $e_{elgn,10}/e_{elgn}$ and $e_{elgn,20}/e_{elgn}$ are 1.37 and 1.24, respectively. The mean values of the ratios for $e_{elgn,10}/e_{elgn}$ and $e_{elgn,20}/e_{elgn}$ are identical of 1.09 and 1.09, respectively, with the corresponding COV of 0.112 and 0.127. The average ratio of elongations for $e_{elgn,20}/e_{elgn,10}$ is 1.00. This may indicate that the higher strain rate was performed on the carbon steel bolted connection tests, the higher elongations corresponding to the ultimate strengths could be obtained. However, by increasing the strain rates from 10 mm/min to 20 mm/min, generally has little effect on the elongations corresponding to the ultimate loads of the carbon steel bolted connections. While for stainless steel bolted connections, it is found that the mean value of the ratios for $e_{elgn,20}/e_{elgn}$ is 1.11, with the corresponding COV of 0.357. The value of $e_{elgn,20}/e_{elgn}$ for stainless steel is 2% higher than that for carbon steel. This may be due to the ductility of stainless steel is higher than those of carbon steel in this study (See the material properties in Table 4). The more ductile of materials could yield more elongations of bolt hole at ultimate load for the bearing failure of connection plate, as compared the bolted connection specimens fabricated by stainless steel with those fabricated by carbon steel. It should be noted that the connection specimens were generally failed by bearing of the connection plates. However, the maximum value of $e_{elgn,20}/e_{elgn}$ is 1.80 for stainless steel bolted connections, i.e., this value of $e_{elgn,20}/e_{elgn}$ for specimen Series D-L-1-12, which is much larger than those of other specimen series. More tests on the stainless steel bolted connection tests under higher strain rates are needed to justify the findings.

4.3 Failure modes

The failure modes of carbon steel and stainless steel bolted connections obtained from the tests are shown in Tables 7-8. As mentioned earlier, all the connection specimens were failed in bearing failure of the connection plates, except for specimen Series S-190-190-2-6 that failed

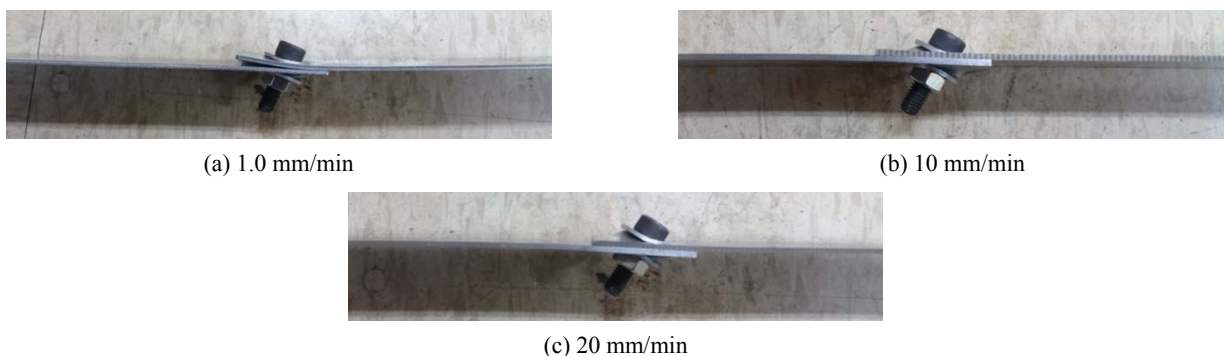


Fig. 14 Bearing failure mode of specimen Series S-190-190-1-8 under different strain rates



Fig. 15 Bearing failure of specimen Series D-120-1-8 under different strain rates

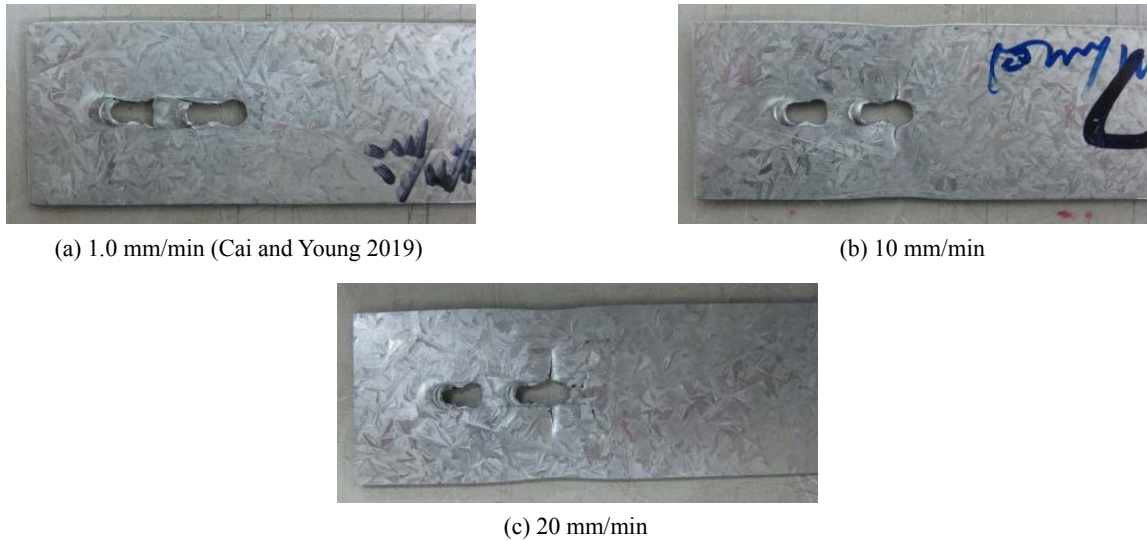


Fig. 16 Failure modes of specimen Series D-190-2-6 under different strain rates



Fig. 17 Bearing failure mode of specimen Series D-A-1-10 under different strain rates

in BS and specimen series D-190-1-10, D-190-2-6 and D-L-2-8 failed by NS failure mode. It is found that the failure modes of carbon steel and stainless steel bolted connections in both single shear and double shear are generally identical despite that the specimens were tested under different strain rates. The strain rates increased from 1.0 mm/min to 20 mm/min generally have no effect on the failure modes of

the carbon steel bolted connection specimens in both single shear and double shear. Similarly, the strain rates increased from 1.5 mm/min to 20 mm/min generally have no effect on the failure modes of the stainless steel bolted connection specimens in both single shear and double shear. The failure modes of carbon steel and stainless steel bolted connection specimens under different strain rates are illustrated in Figs.

14-17 for specimen series S-190-190-1-8, D-120-1-8, D-190-2-6 and D-A-1-10, respectively.

5. Comparison of test results with predictions

5.1 General

Design rules for cold-formed carbon steel bolted connections are provided in the current international specifications, including the Australian/New Zealand Standard (AS/NZS4600 2018) for Cold-formed Steel Structures, Eurocode3 - Design of Steel Structures - Part 1.3 (EC3-1.3 2006): General Rules - Supplementary Rules for Cold-formed Members and Sheeting and the North American Specification (AISI S100 2016) for the Design of Cold-formed Steel Structural Members. The design rules for stainless steel bolted connections are based on the following specifications, including the American Society of Civil Engineers Specification (ASCE 2002) for the Design of Cold-formed Stainless Steel Members, the Australian/New Zealand Standard (AS/NZS4673 2001) for Cold-formed Stainless Steel Structures and the Eurocode 3 - Design of Steel Structures - Part 1.4 (EC3-1.4 2015): General Rules - Supplementary Rules for Stainless Steels. It should be noted that the EC3-1.4 (2015) mainly refers to the design rules in Eurocode 3: Design of Steel Structures - Part 1.8: Design of Joints (EC3-1.8 2005). The design equations for stainless steel bolted connection in the ASCE (2002) are identical to those in the AS/NZS4673 (2001). Hence, the predictions for stainless steel bolted connections by ASCE (2002) and

AS/NZS4673 (2001) are identical.

The above design specifications are used to calculate the nominal strengths (unfactored design strengths) of the carbon steel and stainless steel bolted connection specimens in this study. Different failure modes for carbon steel and stainless steel bolted connections are specified in the design specifications. Different failure modes are associated with the different design equations. Hence, the minimum nominal strength is taken as the predicted strength of a bolted connection and, correspondingly, the predicted failure mode. A bolted connection specimen subjected to tensile loading may fail in the bolt by bolt shear (BS) or combined shear and tension, or fail in the connection plate by bearing (B), tearout (shear rupture) or net section tension (tension rupture). It should be noted that in the Section A3.1.2 of the NAS (2016), if steels with $3\% \leq \text{elongation} < 10\%$, a reduced yield stress of $0.9f_{0.2}$ and the tensile strength of $0.9f_u$ should be used in place of $f_{0.2}$ and f_u , respectively. Hence, the reduced material yield stress and tensile strength of carbon steel 1.20 mm G500 were used in the calculation. The differences of the design equations for different failure modes and the differences among the different design specifications are discussed by Yan and Young (2011) for carbon steel bolted connections, and by Cai and Young (2014a) for stainless steel bolted connections.

5.2 Ultimate loads

The predicted strength was determined by the minimum nominal strength of a bolted connection by considering different failure modes, for carbon steel bolted connections

Table 10 Comparison of test strengths with predictions for carbon steel bolted connections

Specimen series	AS/NZS4600 (2018)			EC3-1.3 (2006)			AISI S100 (2016)		
	P_u/P_1^*	$P_{u,10}/P_1$	$P_{u,20}/P_1$	P_u/P_2^*	$P_{u,10}/P_2$	$P_{u,20}/P_2$	P_u/P_3^*	$P_{u,10}/P_3$	$P_{u,20}/P_3$
S-120-120-1-8	0.99	1.07	1.08	1.19	1.28	1.31	1.10	1.19	1.20
S-120-120-1-10	0.86	0.87	0.95	1.04	1.05	1.15	0.95	0.97	1.05
S-120-120-1-10-R	-	0.89	-	-	1.07	-	-	0.99	-
S-120-190-1-8	1.10	1.08	1.09	1.33	1.31	1.31	1.22	1.21	1.21
S-120-190-1-10	0.95	1.04	1.02	1.14	1.26	1.24	1.05	1.16	1.13
S-190-190-1-8	1.08	1.12	1.12	1.30	1.34	1.35	1.08	1.12	1.12
S-190-190-1-10	0.95	0.96	1.03	1.14	1.16	1.23	0.95	0.96	1.03
S-120-120-2-6	0.99	0.97	1.01	1.20	1.17	1.22	1.10	1.08	1.12
S-120-190-2-6	1.04	1.06	1.08	1.26	1.29	1.31	1.15	1.18	1.20
S-190-190-2-6	-	-	-	-	-	-	-	-	-
D-120-1-8	0.89	0.94	0.90	1.44	1.51	1.43	0.99	1.05	0.99
D-120-1-10	0.97	0.82	0.97	1.29	1.32	1.30	0.99	1.01	1.00
D-190-1-8	1.07	1.14	1.14	1.71	1.82	1.83	1.07	1.14	1.14
D-190-1-10	1.18	1.20	1.20	1.57	1.59	1.59	1.09	1.11	1.11
D-120-2-6	1.07	1.08	1.09	1.31	1.32	1.34	1.11	1.11	1.13
D-190-2-6	1.16	1.20	1.22	1.42	1.47	1.48	1.08	1.12	1.13
Mean	1.02	1.03	1.06	1.31	1.33	1.36	1.07	1.09	1.11
COV	0.094	0.114	0.086	0.137	0.152	0.129	0.072	0.074	0.063

*Note: Detailed in Cai and Young (2019)

(AS/NZS4600 2018, EC3-1.3 2006 and AISI S100 2016) and stainless steel bolted connections (ASCE 2002, EC3-1.4 2015). It should be noted that for the same specimen series tested at different strain rates, the design equations are identical in each design specification. In other words, the effects of strain rate are not considered in the design equations in the aforementioned design specifications for either cold-formed steel or stainless steel. The symbols of P_1 , P_2 , P_3 , P_4 and P_5 represent the strengths (unfactored strength) predicted by AS/NZS4600 (2018), EC3-1.3 (2006), AISI S100 (2016), ASCE (2002) and EC3-1.4 (2015), respectively. The test strengths were compared with the predicted strengths in this study. Note that bolt shear failure was deliberately avoided in the specimen design, and this failure mode was not observed in the test results expect for specimen Series S-190-190-2-6 (See Table 9). The test strengths of the specimen Series S-190-190-2-6 were not included in the comparison due to the actual material properties of the bolts were not tested. As mentioned previously, this study mainly focused on the bolted connections that failed in bearing failure (B) of the connection plates.

Table 10 shows the comparisons between the test strengths and the predicted strengths for the carbon steel bolted connections. It is shown that the AS/NZS4600 (2018), EC3-1.3 (2006) and AISI S100 (2016) generally provide conservative predictions for all the series of connections, where AS/NZS4600 (2018) and the EC3-1.3 (2006) provide the least conservative and most conservative predictions, respectively, e.g., the mean values of P_u/P_1 , P_u/P_2 and P_u/P_3 for carbon steel bolted connections are 1.02, 1.31 and 1.07, respectively. However, the AISI S100 (2016) provides the least scattered predictions, e.g., the coefficients of variation (COV) corresponding to the P_u/P_1 , P_u/P_2 and P_u/P_3 are 0.094, 0.137 and 0.072, respectively. It should be noted that predictions by EC3-1.3 (2006) are conservative for all the series of connections, as the values of P_u/P_2 , $P_{u,10}/P_2$ and $P_{u,20}/P_2$ are all larger than 1.00 (see Table 10). The predictions become more conservative for the specimens tested at higher strain rates; this is because the higher test strengths were generally associated with the higher strain rates as mentioned previously. Figs. 18-20

illustrate the comparison between the test strengths and the prediction strengths for AS/NZS4600 (2018), EC3-1.3 (2006) and AISI S100 (2016), respectively. The legends “S” and “D” in the figures mean single shear and double shear bolted connection specimens, respectively.

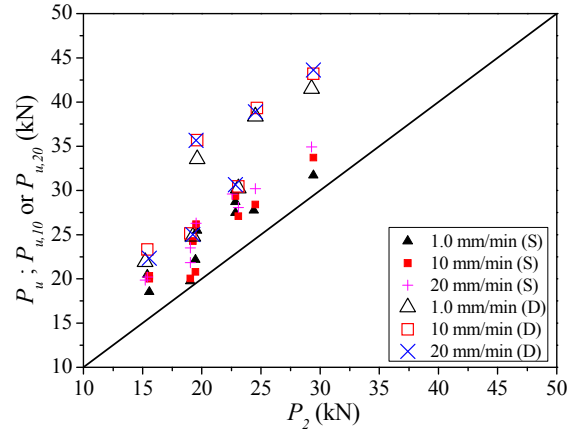


Fig. 19 Comparison of test strengths of carbon steel with predicted strengths by EC3-1.3 (2006)

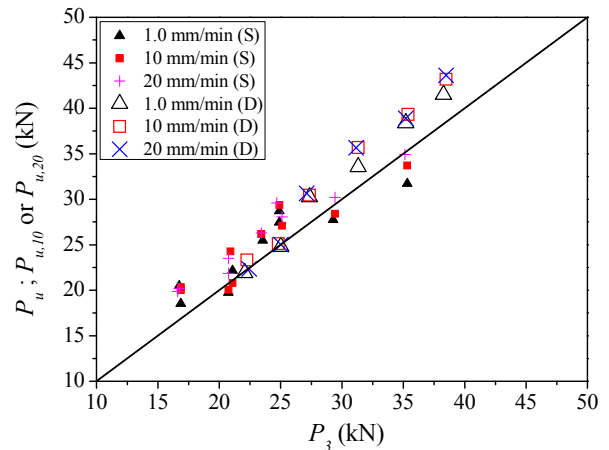


Fig. 20 Comparison of test strengths of carbon steel with predicted strengths by AISI S100 (2016)

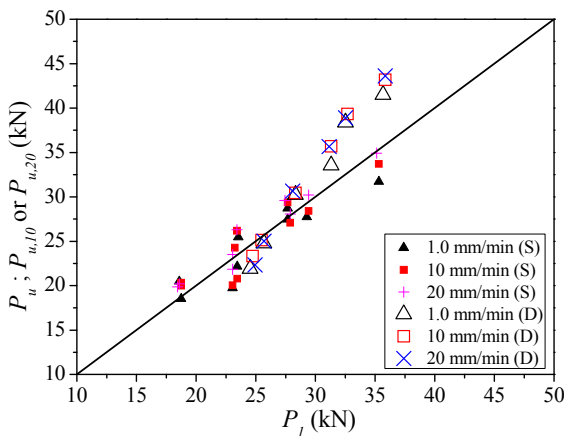


Fig. 18 Comparison of test strengths of carbon steel with predicted strengths by AS/NZS4600 (2018)

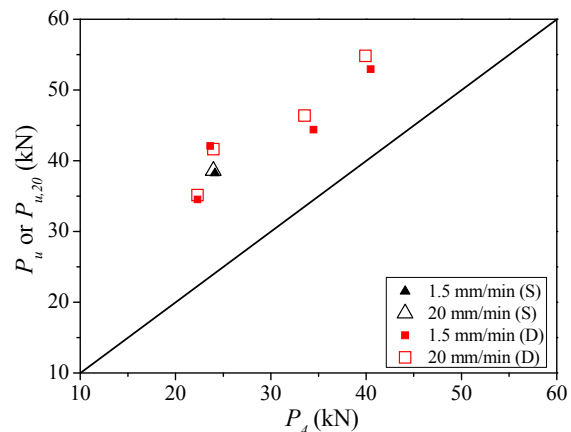


Fig. 21 Comparison of test strengths of stainless steel with predicted strengths by ASCE (2002)

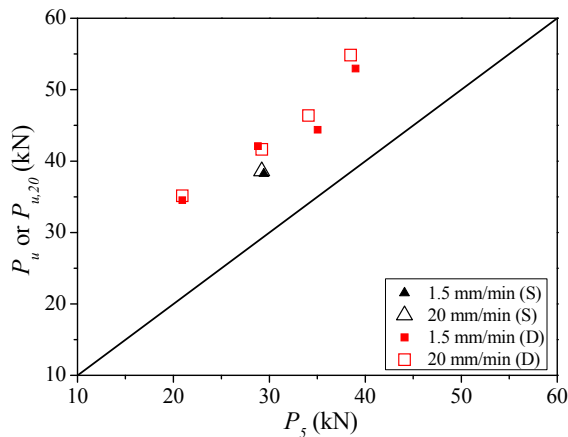


Fig. 22 Comparison of test strengths of stainless steel with predicted strengths by EC3-1.4 (2015)

For stainless steel bolted connections (see Table 11), both the ASCE (2002) and EC3-1.4 (2015) provide conservative predictions for all the connection series. On contrary to the findings for the carbon steel bolted connections, the predictions by EC3-1.4 (2015) are less conservative and less scattered than those predicted by the ASCE (2002), e.g., the mean values of P_u/P_4 and P_u/P_5 are 1.50 and 1.41 with the corresponding COV of 0.137 and 0.110. It should be noted that the design equations for stainless steel bolted connections provided by the ASCE (2002) and AS/NZS4673 (2001) are identical. Hence, their predictions are identical. Similar to those of carbon steel bolted connections, the predictions become more conservative for the specimens tested at higher strain rates due to the resulted higher test strengths, e.g., the mean values of P_u/P_4 and $P_{u,20}/P_4$ are 1.50 and 1.54, respectively. Figs. 21-22 illustrate the comparison between the test strengths and the prediction strengths for ASCE (2002) and EC3-1.4 (2015), respectively.

5.3 Failure modes

The failure mode associated with the minimum nominal strength for each specimen was taken as the predicted failure mode. The predicted failure modes for the carbon steel and stainless steel bolted connections are shown in Tables 7-8, respectively. As mentioned previously, the effects of strain rate are not considered in the current design equations for bolted connections. Hence, the predictions are not distinguished by the different strain rates.

For carbon steel bolted connections in single shear, it was found that the predicted failure modes by AS/NZS4600 (2018), EC3-1.3 (2006) and AISI S100 (2016) are consistent with the failure modes from the tests conducted at different strain rates, except for specimen Series S-190-190-2-6 that failed in BS and were not included in the comparison. It should be noted that all the single shear bolted connections of carbon steel failed in bearing failure (B) of the connection plates except for specimen Series S-190-190-2-6. While for carbon steel double shear bolted connections, the predicted failure mode by EC3-1.3 (2006) is in B for all specimens, which are in consistent with the

Table 11 Comparison of test strengths with predictions for stainless steel bolted connections

Specimen series	ASCE (2002)		EC3-1.4 (2015)	
	P_u/P_4^*	$P_{u,20}/P_4$	P_u/P_5^*	$P_{u,20}/P_5$
S-A-2-8	1.59	1.61	1.30	1.32
D-A-1-10	1.55	1.57	1.65	1.68
D-L-1-12	1.29	1.38	1.27	1.36
D-A-2-8	1.78	1.74	1.46	1.42
D-L-2-8	1.31	1.37	1.36	1.43
Mean	1.50	1.54	1.41	1.44
COV	0.137	0.102	0.110	0.097

*Note: Detailed in Cai and Young (2019)

test results conducted at lower strain rate of 1.0 mm/min. However, it should be noted that the failure mode of B at lower strain rate (1.0 mm/min) transferred to failure mode of NS at higher strain rates (10 mm/min and 20 mm/min), for specimen series D-190-1-10 and D-190-2-6. The predicted failure modes by AS/NZS4600 (2018) and AISI S100 (2016) are identical for all the specimens. The predicted NS failure mode by AS/NZS4600 (2018) and AISI S100 (2016) is consistent with the failure mode of specimen series D-190-1-10 and D-190-2-6 conducted at higher strain rates. However, the predicted failure mode of NS (AS/NZS4600 2018 and AISI S100 2016) is inconsistent with the tested failure mode for specimen series D-120-1-10 and D-120-2-6.

For the stainless steel single shear and double shear bolted connections (see Table 8), the failure mode predicted by the ASCE (2002) is NS failure for all the specimens, which are generally inconsistent with the failure modes from the tests. Note that all the stainless steel single shear and double shear bolted connections failed in B, except for Specimen D-L-2-8 tested at the strain rate of 20 mm/min. The failure modes predicted by the EC3-1.4 (2015) are more consistent with the test results compared with those predicted by the ASCE (2002). The predicted failure mode of B by EC3-1.4 (2015) for specimen series D-A-1-10 and D-L-1-12 is consistent with the test results conducted at different strain rates, and failure mode of NS is consistent with Specimen D-L-2-8 tested at the strain rate of 20 mm/min. The different predictions of failure mode associated with the design equations in different design specifications (ASCE 2002, EC3-1.4 2006) were discussed by Cai and Young (2014a).

6. Conclusions

Experimental investigations on the behaviour of carbon steel and stainless steel bolted connections were conducted. The connection specimens were fabricated from carbon steel grades 1.20 mm G500 and 1.90 mm G450, as well as cold-formed stainless steel types EN 1.4301 and EN 1.4162 with nominal thickness 1.50 mm. Totally 36 bolted connection specimens were designed and tested, which varied in plate thickness, steel grades, bolt diameters, bolt

numbers and connection types. The connection tests were conducted by displacement control test method. The strain rates of 10 mm/min and 20 mm/min were used for carbon steel bolted connections, while the strain rate of 20 mm/min was used for stainless steel bolted connections.

Structural behaviour of the connection specimens undergoing different strain rates was investigated in terms of ultimate load, elongation corresponding to ultimate load and failure mode. Generally, it is shown that the higher strain rate was performed, the higher ultimate loads were obtained for both carbon steel and stainless steel bolted connections. The ultimate loads were averagely 2-5% higher, while the corresponding elongations were averagely 9-11% higher when the test results obtained from the higher strain rate of 20 mm/min compared with those obtained from the lower strain rates (1.0 mm/min for carbon steel and 1.5 mm/min for stainless steel). The effects of strain rates on the ultimate loads of stainless steel bolted connections were generally less significant than those of carbon steel bolted connections. The carbon steel and stainless steel bolted connection specimens were generally failed bearing failure of the connection plates. It is shown that increasing the strain rate up to 20 mm/min generally has no effect on the bearing failure mode of the carbon steel and stainless steel bolted connections.

The test strengths and failure modes were compared with the results predicted by the bolted connection design rules in current international design specifications, including AS/NZS4600 (2018), EC3-1.3 (2006) and AISI S100 (2016) for cold-formed carbon steel as well as ASCE (2002), AS/NZS4673 (2001) and EC3-1.4 (2015) for stainless steel. It is shown that the AS/NZS4600 (2018), EC3-1.3 (2006) and AISI S100 (2016) generally provide conservative predictions for the carbon steel bolted connections, where AS/NZS4600 (2018) and EC3-1.3 (2006) respectively provide the least conservative and most conservative predictions. It was also found that both the ASCE (2002) and the EC3-1.4 (2015) provide conservative predictions for the stainless steel bolted connections. The predictions for both carbon steel and stainless steel bolted connections become more conservative for the specimens tested at higher strain rates due to the resulted higher tested strengths. In terms of failure modes, it was found that the EC3-1.3 (2006) generally provide more accurate predictions than the AS/NZS4600 (2018) and the AISI S100 (2016) for carbon steel bolted connections; while for stainless steel bolted connections, the failure modes predicted by the EC3-1.4 (2015) are more consistent with the test results compared with those predicted by the ASCE (2002).

Acknowledgments

The authors are grateful to BlueScope Lysaght (Singapore) Pte. Ltd. and STALA Tube Finland for supplying the test specimens. The research work described in this paper was supported by a grant from the Research Grants Council of the Hong Kong Special Administrative Region, China (Project No. HKU719711E).

References

- Agheshlui, H., Goldsworthy, H., Gad, E. and Mirza, O. (2017), "Anchored blind bolted composite connection to a concrete filled steel tubular column", *Steel Compos. Struct., Int. J.*, **23**(1), 115-130.
- AISI S100 (2016), North American Specification for the Design of Cold-Formed Steel Structural Members; American Iron and Steel Institute, *AISIS 100-2016*, AISI Standard.
- ASCE (2002), Specification for the design of cold-formed stainless steel structural members; American Society of Civil Engineers (ASCE), ASCE Standard, *SEI/ASCE-8-02*, Reston, VA, USA.
- AS/NZS4673 (2001), Cold-formed stainless steel structures; AS/NZS 4673:2001, Australian/New Zealand Standard (AS/NZS), Standards Australia, Sydney, Australia.
- AS/NZS4600 (2018), Cold-formed Steel Structures; Australian/New Zealand Standard, AS/NZS4600:2018, Sydney, Australia, Standards Australia.
- AS1391 (2007), Metallic materials—Tensile testing at ambient temperature; AS1391:2007, Standards Australia, Sydney, Australia.
- Boh, J.W., Louca, L.A. and Choo, Y.S. (2004), "Strain rate effects on the response of stainless steel corrugated firewalls subjected to hydrocarbon explosions", *J. Constr. Steel Res.*, **60**, 1-29.
- Bouchair, A., Averseng, J. and Abidelah, A. (2008), "Analysis of the behaviour of stainless steel bolted connections", *J. Constr. Steel Res.*, **64**(11), 1264-1274.
- Cai, Y. and Young, B. (2014a), "Structural behavior of cold-formed stainless steel bolted connections", *Thin-Wall. Struct.*, **83**, 147-156.
- Cai, Y. and Young, B. (2014b), "Behavior of cold-formed stainless steel single shear bolted connections at elevated temperatures", *Thin-Wall. Struct.*, **75**, 63-75.
- Cai, Y. and Young, B. (2014c), "Transient state tests of cold-formed stainless steel single shear bolted connections", *Eng. Struct.*, **81**, 1-9.
- Cai, Y. and Young, B. (2015), "High temperature tests of cold-formed stainless steel double shear bolted connections", *J. Constr. Steel Res.*, **104**, 49-63.
- Cai, Y. and Young, B. (2018), "Bearing resistance design of stainless steel bolted connections at ambient and elevated temperatures", *Steel Compos. Struct., Int. J.*, **29**(2), 273-286.
- Cai, Y. and Young, B. (2019), "Carbon steel and stainless steel bolted connections undergoing unloading and re-loading processes", *J. Constr. Steel Res.*, **157**, 337-346.
- Chung, K.F. (2005), "Structural performance of cold-formed steel structures with bolted connections", *Adv. Struct. Eng.*, **8**(3), 231-245.
- De Nardin, S. and El Debs, A.L.H.C. (2018), "Shear transfer mechanism in connections involving concrete filled steel columns under shear forces", *Steel Compos. Struct., Int. J.*, **28**(4), 449-460.
- Esaki, F. and Ono, M. (2001), "Effects of loading rate on mechanical behavior of SRC shear walls", *Steel Compos. Struct., Int. J.*, **1**(2), 201-212.
- EC3-1.3 (2006), Eurocode 3 - Design of Steel Structures - Part 1.3: General Rules Supplementary Rules for Cold-formed Members and Sheeting; European Committee for Standardization, *EN1993-1-3:2006*, Brussels, Belgium.
- EC3-1.4 (2015), Eurocode 3 - Design of steel structures - Part 1.4: General rules - Supplementary rules for stainless steels; *EN 1993-1-4:2006+A1:2015*, European Committee for Standardization, Brussels, Belgium.
- EC3-1.8 (2005), Eurocode 3 - Design of steel structures—Part 1.8: Design of joints; European Committee for Standardization, *BS EN 1993-1-8:2005*, CEN, Brussels, Belgium.

- El Hassouni, A., Plumier, A. and Cherrabi, A. (2011), "Experimental and numerical analysis of the strain-rate effect on fully welded connections", *J. Constr. Steel Res.*, **67**(3), 533-546.
- Girhammar, U.A. and Andersson, H. (1988), "Effect of loading rate on nailed timber joint capacity", *J. Struct. Eng.*, **114**(11), 2439-2456.
- Grimsmo, E.L., Clausen, A.H., Langseth, M. and Aalberg, A. (2015), "An experimental study of static and dynamic behavior of bolted end-plate joints of steel", *Int. J. Impact Eng.*, **85**, 132-145.
- Jones, N. (1997), *Structural impact*, Cambridge University Press Cambridge, UK.
- Kazemi, K.S.M., Sohrabi, M.R. and Kazemi, H.H. (2018), "Evaluation the behavior of pre-fabricated moment connection with a new geometry of pyramidal end block under monotonic and cyclic loadings", *Steel Compos. Struct., Int. J.*, **29**(3), 391-404.
- Kim, T.S. and Kuwamura, H. (2007), "Finite element modeling of bolted connections in thin-walled stainless steel plates under static shear", *Thin-Wall. Struct.*, **45**(4), 407-421.
- Li, D., Uy, B., Patel, V. and Aslani, F. (2016), "Behaviour and design of demountable steel column-column connections", *Steel Compos. Struct., Int. J.*, **22**(2), 429-448.
- Li, G.-Q., Gu, F., Jiang, J. and Sun, F. (2017a), "Cyclic behavior of steel beam-concrete wall connections with embedded steel columns (I): Experimental study", *Steel Compos. Struct., Int. J.*, **23**(4), 399-408.
- Li, G.-Q., Gu, F., Jiang, J. and Sun, F. (2017b), "Cyclic behavior of steel beam-concrete wall connections with embedded steel columns (II): Theoretical study", *Steel Compos. Struct., Int. J.*, **23**(4), 409-420.
- Li, S., Li, Q., Jiang, H., Zhang, H., Yan, L. and Jiang, W. (2018), "Experimental study on a new type of assembly bolted end-plate connection", *Steel Compos. Struct., Int. J.*, **26**(4), 463-471.
- Lu, G.X. and Yu, T.X. (2003), "Energy absorption of structures and materials", Woodhead Publishing, Oxford, UK.
- Pan, C.L., Wu, S. and Yu, W.W. (2001), "Strain rate and aging effect on the mechanical properties of sheet steels", *Thin-Wall. Struct.*, **39**, 429-444.
- Rathnaweera, G., Durandet, Y., Ruan, D. and Kinoshita, S. (2011), "Characterizing the material properties of a tube from a lateral compression test", *Int. J. Protect. Struct.*, **2**(4), 465-476.
- Rogers, C.A. and Hancock, G.J. (1998), "Bolted connection tests of thin G550 and G300 sheet steels", *J. Struct. Eng.*, **124**(7), 798-808.
- Rogers, C.A. and Hancock, G.J. (1999), "Bolted connection design for sheet steels less than 1.0 mm thick", *J. Constr. Steel Res.*, **51**(2), 123-146.
- Salih, E.L., Gardner, L. and Nethercot, D.A. (2010), "Numerical investigation of net section failure in stainless steel bolted connections", *J. Constr. Steel Res.*, **66**(12), 1455-1466.
- Salih, E.L., Gardner, L. and Nethercot, D.A. (2011), "Bearing failure in stainless steel bolted connections", *Eng. Struct.*, **33**(2), 549-562.
- Soroushian, P. and Choi, K.B. (1987), "Steel mechanical properties at different strain rates", *J. Struct. Eng.*, **113**(4), 663-672.
- Teh, L.H. and Clements, D.D.A. (2012), "Block shear capacity of bolted connections in cold-reduced steel sheets", *J. Struct. Eng.*, **138**(4), 459-467.
- Teh, L.H. and Uz, M.E. (2015), "Ultimate shear-out capacities of structural-steel bolted connections", *J. Struct. Eng.*, **141**(6), 04044152.
- Vatansever, C. and Kutsal, K. (2018), "Effect of bolted splice within the plastic hinge zone on beam-to-column connection behaviour", *Steel Compos. Struct., Int. J.*, **28**(6), 767-778.
- Yan, S. and Young, B. (2011), "Tests of single shear bolted connections of thin sheet steels at elevated temperatures —Part I: steady state tests", *Thin-Wall. Struct.*, **49**, 1320-1333.
- Yan, S. and Young, B. (2012), "Bearing factors for single shear bolted connections of thin sheet steels at elevated temperatures", *Thin-Wall. Struct.*, **52**, 126-142.
- Yan, S. and Young, B. (2013), "Effects of Elevated Temperatures on Double Shear Bolted Connections of Thin Sheet Steels", *J. Struct. Eng.*, **139**, 757-771.
- Yuen, S.C.K., Nurick, G.N. and Witbeen, H.L. (2011), "The response of sandwich panels made of thin-walled tubes subjected to axial load", *Int. J. Protect. Struct.*, **2**(4), 477-498.
- Zeinoddini, M., Parke, G.A.R. and Harding, J.E. (2002), "Axially pre-loaded steel tubes subjected to lateral impacts: an experimental study", *Int. J. Impact Eng.*, **27**(6), 669-690.
- Zeinoddini, M., Harding, J.E. and Parke, G.A.R. (2008), "Axially pre-loaded steel tubes subjected to lateral impacts (a numerical simulation)", *Int. J. Impact Eng.*, **35**(11), 1267-1279.

DL